Temperature Dependence of Structure, Bending Rigidity, and Bilayer Interactions of Dioleoylphosphatidylcholine Bilayers

Jianjun Pan,* Stephanie Tristram-Nagle,* Norbert Kučerka,[‡§] and John F. Nagle*[†]

*Department of Physics, and [†]Department of Biological Sciences, Carnegie Mellon University, Pittsburgh, Pennsylvania; [‡]Canadian Neutron Beam Centre, National Research Council, Chalk River, Ontario, Canada; and [§]Department of Physical Chemistry of Drugs, Faculty of Pharmacy, Comenius University, Bratislava, Slovakia

ABSTRACT X-ray diffuse scattering was measured from oriented stacks and unilamellar vesicles of dioleoylphosphatidylcholine lipid bilayers to obtain the temperature dependence of the structure and of the material properties. The area/molecule, A, was 75.5 Å^2 at 45°C, 72.4 Å^2 at 30°C, and 69.1 Å^2 at 15°C, which gives the area expansivity $\alpha_A = 0.0029$/deg at 30°C, and we show that this value is in excellent agreement with the polymer brush theory. The bilayer becomes thinner with increasing temperature; the contractivity of the hydrocarbon portion was $\alpha_{Dc} = 0.0019$/deg; the difference between α_A and α_{Dc} is consistent with the previously measured volume expansivity $\alpha_{Vc} = 0.0010$/deg. The bending modulus K_C decreased as exp(455/T) with increasing T (K). Our area compressibility modulus K_A decreased with increasing temperature by 5%, the same as the surface tension of dodecane/water, in agreement again with the polymer brush theory. Regarding interactions between bilayers, the compression modulus B as a function of interbilayer water spacing D_W' was found to be nearly independent of temperature. The repulsive fluctuation pressure calculated from B and K_C increased with temperature, and the Hamaker parameter for the van der Waals interaction was nearly independent of temperature; this explains why the fully hydrated water spacing, D_W', that we obtain from our structural results increases with temperature.

INTRODUCTION

Many investigators have studied the effects of chain length and chain unsaturation on bilayer properties and structure (1–5). Such studies provide the fundamental basis for understanding the organization of biomembranes, including interactions between membrane proteins and lipids (6,7). One of the most important structural parameters is the area, A, per lipid molecule (8). Reported areas for dioleoylphosphatidylcholine (DOPC) include 72.1 Å^2 at 30°C (9), 59.3 Å^2 at 23°C (10), 70.1 Å^2 at 22°C (11), and 70 Å^2 at 2°C (12). Comparison of these results is problematic unless the results can be adjusted for the temperature differences. By obtaining results at several different temperatures, thermal derivatives can be estimated and then used to adjust results obtained at one temperature.

Extensive structural results as a function of temperature have been reported for phospholipids with saturated hydrocarbon chains (2) using NMR techniques that are not easily applicable to lipids with unsaturated chains, so our study focuses on the most studied, benchmark, unsaturated lipid, DOPC, that has one double bond at the 9–10 position of both the *sn*-1 and *sn*-2 chains. The temperature dependence of DOPC has been studied using the Luzzati gravimetric x-ray method (13). The temperature dependence of egg phosphatidylcholine (eggPC) has been studied with low-resolution x-ray diffraction (14) and that of dimyristoylphosphatidylcholine (DMPC) by low-resolution neutron scattering (15). Detailed comparisons to all these previous results will be made.

The electron density profile (EDP) of lipid bilayers that is obtained from x-ray studies and the associated structural inferences that can then be drawn are of basic interest in membrane biophysics. Earlier liquid-crystallographic x-ray studies from this lab have been reviewed (8). More recent studies (16) provide twice the spatial resolution in the fully hydrated fluid (L_α) phase by taking advantage of the diffuse scattering inherent in such disordered systems that provides more information than the traditional liquid crystallographic approach. Although both our second- and third-millennium works have reported results for several different lipids, neither have yet addressed the temperature dependence of any lipid bilayer in its fluid phase. That is the focus of this article.

Our diffuse scattering methodology also obtains mesoscopic material properties, such as the bending modulus, K_C, that governs undulational fluctuations and the bulk modulus, B, that provides information about the interactions between bilayers. The bending modulus K_C and the closely associated area compression modulus, K_A, have been reported for many lipids at 21°C and a polymer brush model for the elasticity and thickness of membranes has been proposed (1). The temperature dependence of these quantities reported in this article is a different experimental dimension to test the polymer brush theory, as well as theories of interaction between membranes (17).

MATERIALS AND METHODS

Synthetic DOPC (1,2-dioleoyl-*sn*-3-phosphocholine) was purchased in lyophilized form from Avanti Polar Lipids (Alabaster, AL) and used as received.

Submitted June 20, 2007, and accepted for publication August 20, 2007.

Address reprint requests to John F. Nagle, Dept. of Physics, Carnegie Mellon University, Pittsburgh, PA 15213. Tel.: 412-268-2764, Fax: 412-681-0648; E-mail: nagle@cmu.edu.

Editor: Lukas K. Tamm.

0006-3495/08/01/117/08 $2.00

doi: 10.1529/biophysj.107.115691

Unilamellar vesicles (ULV)

Following our usual procedure (18), 10 mg DOPC was added to 500 μl Barnstead nanopure water in a nalgene plastic vial and then hydrated by repetitive cycles of heating and cooling until the multilamellar vesicles were uniformly dispersed. The ULV samples were obtained by passing the multilamellar vesicles through an Avanti miniextruder 25 times, using polycarbonate filters with 500-Å-diameter pores, followed by centrifugation to remove remaining multilamellar vesicles. The time between sample preparation and x-ray experiment at the Cornell High Energy Synchrotron Source (CHESS) was not more than 10 h. Before exposure to x-rays, the ULV sample was poured into a circular lumen 1.5 mm thick along the beam. The average size is 600 Å in diameter, which is obtained by dynamic light scattering and neutron scattering of similarly prepared vesicles (19).

Oriented samples

Following our usual procedure (18), 4 mg of DOPC lipid was added to a chloroform/trifluoroethanol (1:1, v/v) mixture. After pouring onto a 15 × 30 × 1-mm clean silicon wafer within a glove box, the organic solvent evaporated while the sample was subjected to shear force in the rock-and-roll procedure (20). The stack of ~2000 oriented DOPC bilayers was then trimmed to a strip 5 mm in the beam direction. Oriented samples were x-rayed at the CHESS G1 ($\lambda = 1.2742$ Å) and D1 ($\lambda = 1.18018$ Å) stations, where the wavelengths were obtained using multilayer monochromators. The sample to CCD distance was 372 mm with a Flicam CCD (pixel size 0.0698 mm) at the G1 station and 245 mm with a Medoptics CCD (pixel size 0.0472 mm) at the D1 station. Between x-ray exposures, the 30-mm-wide sample was moved laterally after a few minutes exposure to avoid radiation damage (beam width was only 0.3 mm), with shorter times appropriate at the high-flux G-line (~10^{13} photons/s/mm^2). Lipid breakdown, examined by thin layer chromatography, was <0.1%. Hydration through the vapor was facilitated with the help of a Peltier cooler under the sample to lower the temperature of the sample relative to the water vapor (by <0.1°), thereby condensing water onto the sample. Less than fully hydrated D-spacings were obtained by applying less Peltier current and/or during the slow (~1- to 2-h) hydration process. The final lamellar D-spacing was within 1 Å of that obtained from unoriented multilamellar vesicles (MLV) in excess water, which was measured in separate capillary experiments.

Analysis

To obtain an EDP, we analyze its Fourier transform, the form factor $F(q_z)$. For unilamellar vesicles, the formula relating the form factor and the scattering intensity is $I(\mathbf{q}) = |F(q_z)|^2/q_z^2$. For oriented bilayer samples, $I(\mathbf{q}) = S(\mathbf{q})|F(q_z)|^2/q_z$. The method to obtain $S(\mathbf{q})$ has been described (21,22). Basically, the system is composed of a stack of N lipid bilayers. The average structure can be described as a one-dimensional array of lipid bilayers, and each of the bilayers is a two-dimensional in-plane fluid. The fluctuation of the bilayers is quantitated by $u_n(r)$, which is the spatial deviation from the average nth bilayer position along the normal of the stack. From smectic liquid crystal theory (23), the free energy function is

$$F_{fl} = \frac{1}{2}\int d\mathbf{r} \sum_{n=0}^{N-1} \{K_C[\Delta u_n(\mathbf{r})]^2 + B[u_{n+1}(\mathbf{r}) - u_n(\mathbf{r})]^2\}. \quad (1)$$

The first term is the bending energy and the second term is the harmonic approximation to the fluctuational part of the interactions between bilayers (24). The bending modulus K_C and the compression modulus B were obtained by fitting the off-specular scattering intensity to the theory for $S(\mathbf{q})$ derived from Eq. 1 (21,22). The determination of K_C and B provides $S(\mathbf{q})$ which, when divided into $I(\mathbf{q})/q_z$ provides $|F(q_z)|^2$. The undulation correction factors, 1.013, 1.012, and 1.0099 for 45°C, 30°C, and 15°C, respectively, were applied to q_z (5,8).

EDPs, structural parameters, and area (A) were determined by fitting the H2 model (25) to $|F(q_z)|^2$. Three constraints on the model, derived from gel-phase studies (26), include the volume of the headgroup ($V_H = 331$ Å^3), the distance between the phosphate and the Gibbs dividing surface for the hydrocarbon region ($D_{H1} = 4.95$ Å), and the ratio of the terminal methyl volume to the average methylene volume ($r = 2$). Absolute errors, especially in area/molecule, A, depend upon these values and the assumption that they apply to the fluid phase. However, relative errors as a function of temperature are likely to be much smaller, so our suggested uncertainties in quantities that involve taking derivatives are obtained for the above set of assumed values. To provide better comparison of the structure at different temperatures, the widths of the two headgroup Gaussians and the distance between their centers were fixed to the values obtained at $T = 30$°C, where these constraints were not applied. The value of $F(0)$ was determined from volume measurements and the fitted area. The absolute specific volume for DOPC at 30°C has been reported as $V_L = 1302.3$ Å^3 (27), 1302.0 Å^3 (28), and 1303.0 Å^3 (9). The latter reference also obtained the volume expansivity, $\alpha_V = (1/V)(\partial V/\partial T)_\Pi = 80 \pm 3 \times 10^{-5}$/deg, which was used together with V_L at 30°C to obtain the values at other temperatures, as given in Table 1.

RESULTS

Structural parameters

The form factors are shown in Fig. 1. As in previous studies (5,16,18), there is satisfactory agreement of the ULV data and the oriented-sample data in the region of overlap (0.22 Å^{-1} < $q_z \sim <$ 0.26 Å^{-1}); this enables us to combine the data sets to extend over a larger q_z range than would be obtained for either data set alone. The q_z values where $F(q_z)$ passes through zero and changes sign define the boundaries of the scattering lobes. The movement of these zeros to smaller q_z values and the general shrinking of the q_z range of the lobes as temperature decreases are indicative of thickening of the bilayers. The higher flux at G1 station enabled us to obtain data to somewhat higher values of q_z than previously. Nevertheless, when the intensity is small, the fitting to the raw data produces a Gaussian distribution that includes some negative values of $|F(q_z)|^2$ that are shown in Fig. 1 as negative values of $|F(q_z)|$; these must be included in the fitting to avoid biasing the model to overly large values of $|F(q_z)|^2$.

Fig. 2 shows the EDPs that confirm that the DOPC bilayer becomes thinner when the temperature increases by the shift of the positions of the component groups toward the bilayer

TABLE 1 Values of structural and model parameters

	45°C	30°C	15°C
Volume/molecule (Å^3)	1318	1303	1288
$F(0)$	−0.132	0.003	0.150
D-spacing (Å)	63.3*	63.2*	62.8*
Bilayer thickness, D_{HH} (Å)	36.1	36.7	37.6
Hydrocarbon thickness, $2D_C$ (Å)	26.2	26.8	27.7
Area per molecule, A (Å^2)	75.5	72.4	69.1
Interbilayer water spacing, D'_W (Å)	19.2*	18.4*	17.1*
Steric bilayer thickness, D'_B (Å)	44.2	44.8	45.7
Bending ridigity, K_C (10^{-20} J)	7.2	7.6	8.5
Stretch modulus, K_A (mN/m)	252	254	264
λ_{fl} (Å)	6.4	5.9	6.4
Hamaker coefficient, H (10^{-21} J)	5.4	5.4	5.2

*Fully hydrated from MLV samples.

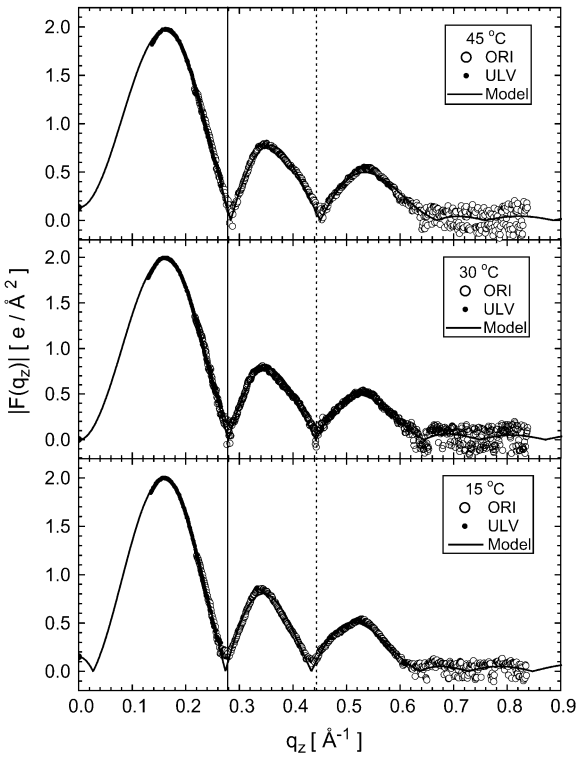

FIGURE 1 Absolute form factor versus q_z. The solid and dotted vertical lines indicate the zeros at 30°C between the first three lobes. The solid black curve shows the model fit.

center. The decrease in the height of the total EDP and also of the headgroup components indicates that the area/lipid, A, increases as temperature increases. Table 1 lists our numerical results for the hydrocarbon chain thickness $2D_C$, the head-head distance, D_{HH}, between the maxima in the EDP, the area per lipid, $A = (V_L - V_H)/D_C$, and the steric bilayer thickness, $D'_B = 2D_C + 18$ Å, assuming 9 Å for each headgroup thickness. Also, the steric water spacing, D'_W, between bilayers is defined as $D - D'_B$ (8). Estimated uncertainties in V, D, and D_{HH} are in the last significant figure in Table 1. Values of A and $2D_C$ depend upon the H2-model assumptions described in Materials and Methods; within that framework, we estimate 1% uncertainties in A and $2D_C$ and in D'_B and D'_W derived from them above.

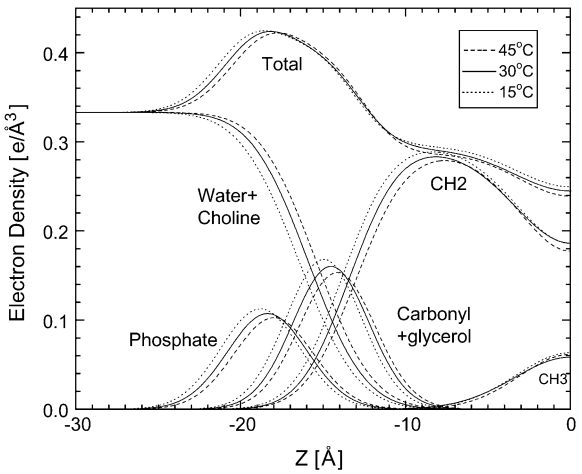

FIGURE 2 Half the symmetric EDP versus distance from the center of the bilayer at $z = 0$. The H2 model (25) is composed of the electron densities of the five components indicated, and the total model electron density is their sum. The unsaturated double bonds in the tails of DOPC are included with the methylene component and the choline is included with the water, because these pairs have similar electron densities.

Fluctuation and interaction parameters

Our results for K_C as a function of temperature and bilayer repeat spacing, D, are shown in Fig. 3. It is clear that K_C doesn't vary with D at a constant temperature when the lamellar repeat spacing increased in the experimental run from its initial mildly dehydrated state to the final, nearly fully hydrated state. We often stopped short of the fully hydrated D-spacing by 1 Å or less because it is possible to raise the relative humidity near the sample above 100%; this floods the sample which disrupts good orientation and causes excess absorption of the beam. However, Fig. 3 shows three data points for $T = 30$°C from one of our runs that had larger D-spacing than our typical fully hydrated MLV sample. Such variations in fully hydrated D-spacings have been discussed (8). The results in Fig. 3 confirm that K_C describes the bending rigidity of a single bilayer, which should not depend upon the interactions with neighboring bilayers that do vary with D. Based on these data, we obtained an average

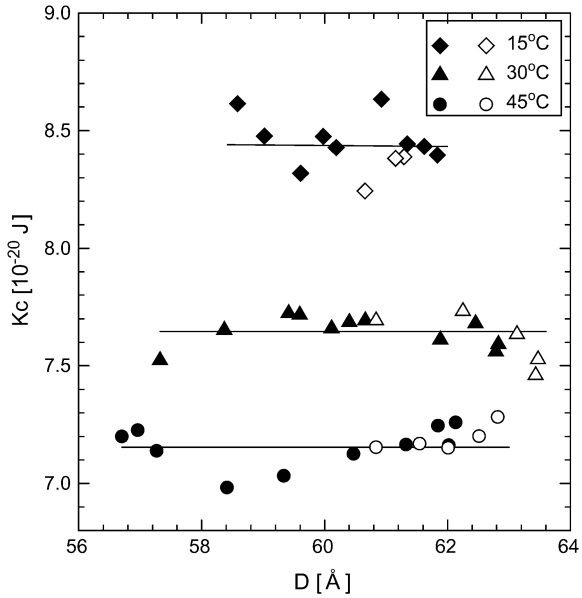

FIGURE 3 Bending rigidity, K_C, versus lamellar repeat spacing, D. The solid horizontal lines are the best estimates for K_C for the three temperatures. The open and solid symbols are from two different synchrotron trips on different beam lines.

value of K_C at each temperature. We also estimated statistical uncertainties of order 0.1×10^{-20} J based on the scatter in the K_C values at each temperature. We note that these statistical uncertainties do not include uncertainties in experimental parameters, such as the angular divergence of the beam and the corresponding coherence lengths, and the correlation lengths of the sample, both in-plane and normal to the stack. As is explained in great detail elsewhere (30), experimental determinations are obtained for these parameters, but their uncertainties nevertheless lead to $\sim 0.5 \times 10^{-20}$ J uncertainties in K_C, which is consistent with the different K_C values of 7.3×10^{-20} J (21), 8.0–8.5 $\times 10^{-20}$ J (22), and 8.0×10^{-20} J (5) that have been reported from this lab for DOPC at 30°C. However, the sample and the experimental setup were the same in each of the two CHESS trips reported in this article, so the corresponding systematic uncertainties, although still present for the absolute values of K_C, are the same for all temperatures and were therefore not used in the evaluation of temperature dependence in K_C. Use of the appropriate uncertainties in the plot in Fig. 4 clearly shows that K_C decreases with increasing temperature. The fit of K_C to $\exp(+\varepsilon_K/kT)$ in Fig. 4 gives $\varepsilon_K = 7 \times 10^{-21}$ J.

From our results for K_C and the hydrocarbon thickness, D_C, we calculate the area compressibility modulus, $K_A = -(\partial A/\partial \Pi)_T/A$ using the formula $K_A = 24K_C/(2D_C)^2$ derived from the polymer brush model (1) with the results shown in Table 1.

Fig. 5 shows our results for the B modulus. The bilayer repeat spacing, D, is converted into an interbilayer water spacing, D'_W, by subtracting steric bilayer thickness (D'_B) from the lamellar repeat spacing, D, for each hydration level. Fig. 5 indicates that there is little temperature dependence in the $B(D'_W)$ curves.

The free energy of the fluctuations (F_{fl}) (both undulations and compression) per unit area was calculated from the formula (24)

$$F_{fl} = \left(\frac{k_B T}{2\pi}\right)\sqrt{\frac{B}{K_C}}, \tag{2}$$

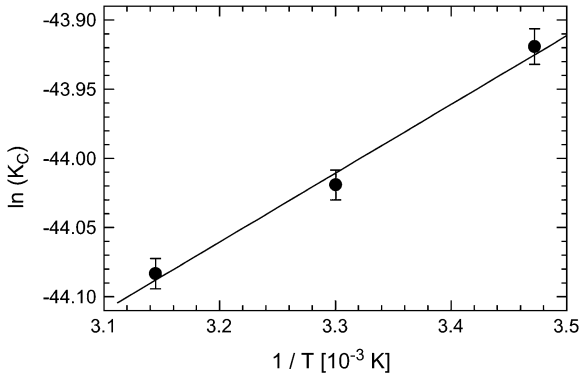

FIGURE 4 Exponential plot for the bending modulus, K_C. The uncertainties were obtained from the fits in Fig. 3.

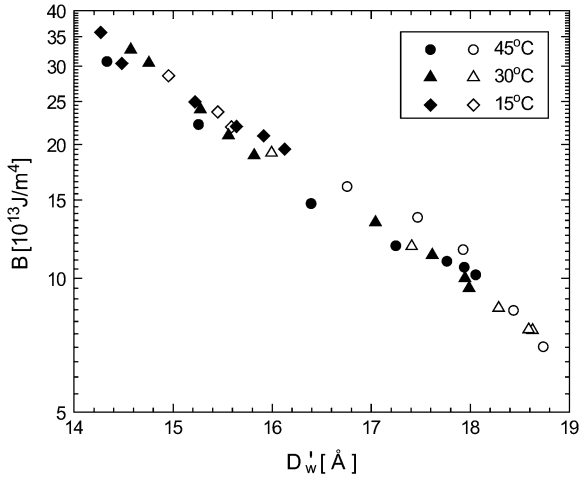

FIGURE 5 Bilayer compression modulus B plotted logarithmically versus interbilayer water spacing D'_W for three temperatures. The open and solid symbols are from different synchrotron trips.

with the results shown on a log plot versus D'_W in Fig. 6. The straight line fits in Fig. 6 imply $F_{fl} \sim \exp(-D'_W/\lambda_{fl})$. Our reported values in Table 1 suggest that λ_{fl} does not vary significantly with temperature within experimental uncertainty. The fluctuation pressure between adjacent bilayers, defined as $P_{fl} = -(\partial F_{fl}/\partial D'_W)_T$, is then given by F_{fl}/λ_{fl}. In addition to this entropic pressure, other pressures are thought to consist of the repulsive hydration pressure,

$$P_{hyd} = P_h \exp(-D'_W/\lambda_h), \tag{3}$$

and the attractive van der Waals pressure (31),

$$P_{vdW} = \frac{H}{6\pi}\left(\frac{1}{D'^3_W} - \frac{2}{D^3} + \frac{1}{(2D - D'_W)^3}\right), \tag{4}$$

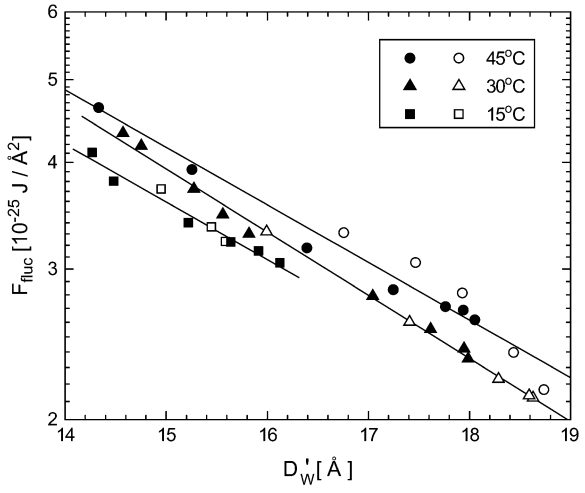

FIGURE 6 Fluctuation free energy plotted logarithmically versus interbilayer water spacing, D'_W. The linear fits give the exponential decay lengths in Table 1.

where H is the Hamaker parameter. The D-spacing is reduced by osmotic pressure $P_{osm} = P_{fl} + P_{hyd} - P_{vdW}$. The total P_{osm} was measured for DOPC at 30°C and it was fitted to the sum of the individual pressures (9). That work permitted determination of P_h and λ_h, but not of H, because only the product of K_C and B could be obtained, so $P_{fl}(D'_W)$ could only be determined to within a factor of K_C. Now that we can determine K_C, P_{fl} is determined by using Eq. 2. Together with the earlier values, $P_h = 0.55 \times 10^8$ J/m^3 and $\lambda_h = 2.2$ Å, obtained at 30°C, we now obtain $H = 5.4 \times 10^{-21}$ J for DOPC. We further assume that the hydration pressure is independent of temperature, as reported by Simon et al. (14). Then the values of D'_W at full hydration together with the requirement that $P_{osm} = 0$ at full hydration enables us to obtain the values of H at 15°C and 45°C that are given in Table 1.

DISCUSSION

Bending rigidity

The value $K_C = 8.5 \pm 1.0 \times 10^{-20}$ J was reported for DOPC at 18°C using the micropipette aspiration technique on giant unilamellar vesicles (1). Interpolation of the values in Fig. 4 to 18°C gives $K_C = 8.2 \times 10^{-20}$ J. The excellent agreement suggests that our oriented samples and our analysis procedure do indeed give the bending modulus K_C for single bilayers.

Our results in Fig. 4 clearly show the intuitively expected result that K_C decreases as temperature increases. Our results also indicate that $K_C(T)$ is not a linear function of temperature. Niggemann et al. (32) used both fluctuation-mode analysis and electric deformation to measure $K_C(T)$ for DOPC, although their absolute values were quite dependent on the different experimental methods and sample preparations. They fit their data to $\exp(\varepsilon_K/kT)$, as we do also (Fig. 4). There are, however, large differences in the results. When expressed in units of thermal energy at $T = 30$°C, they obtained $\varepsilon_K/kT = 25$, corresponding to a decrease in K_C by a factor of 5 between 13°C and 34°C, whereas we obtain $\varepsilon_K/kT = 1.5$, corresponding to a factor of only 1.2 between 15°C and 45°C. Our experience with other samples and the diffuse scattering theory show that the raw CCD data would appear dramatically different to the naked eye if K_C changed by a factor of 5; instead, our CCD images, although they are quantitatively different, are qualitatively similar, consistent with only a factor of 1.2 in the K_C values.

Let us next discuss the values of the area compressibility modulus K_A that we give in Table 1. (Recall that in our study, K_A is derived from K_C, hydrocarbon thickness, $2D_C$, and the polymer-brush-model equation, $K_A = 24K_C/(2D_C)^2$.) When interpolated to 18°C, our $K_A \approx 260$ mN/m is in good agreement with the $K_A = 265 \pm 18$ mN/m directly measured for DOPC at 18°C (1), thereby indicating general consistency of our results and also adding more data to support the factor of 24 in their equation. Rawicz et al. (1) further emphasized that their K_A values were the same in first approximation for many lipids near room temperature. This was foundational to their theory that predicts $K_A = 6\Pi = 6\gamma$ for any lipid bilayer, where γ is essentially the oil/water surface tension. Our data expands the test of this equation by comparing one lipid over a temperature range instead of many lipids at the same temperature. Our K_A for DOPC in Table 1 decreases by ~4.5% from 15°C to 45°C. Between the same two temperatures, γ for hexane/water decreases by 5.1%, and this percentage monotonically decreases as the oil chain length is increased to 4.5% for dodecane (33). This latter percentage is in striking agreement with the thermal decrease of our $K_A(T)$. It may also be noted that the temperature dependence of K_C reported by Niggemann et al. (32) would strongly violate this theory. A considerably smaller disagreement is the decrease in K_A by 30% as temperature was increased by 10% that was reported for a coarse-grained simulation (34).

Structure: expansivities

We report in Table 2 a single number for the area expansivity $\alpha_A = (\partial A/\partial T)_\Pi/A = 0.0029$/deg for $T = 30$°C. Although a substantial temperature dependence in α_A has been shown for DMPC near its phase transition temperature due to subcritical fluctuations (35), such anomalous behavior is not expected for DOPC in the 15°–45°C temperature range which is well above the DOPC phase transition that is near −17°C (36). The polymer brush theory predicts

$$A = 2a_c[3n_s k_B T/a_c\gamma]^{1/3}, \quad (5)$$

where a_c is the area per chain in well-ordered gel phases and n_s is the so-called number of statistical segments per chain. The explicit T dependence in Eq. 5 gives a contribution $(1/A)(\partial A/\partial T) = 1/3T$ to α_A that we will call α_1. The magnitude of α_1 is 0.0011/deg when evaluated at $T = 30$°C. This is much smaller than our measured value. However, α_A must also include the implicit temperature dependencies of the other three variables in Eq. 5. We will name these $\alpha_2 = -(1/3\gamma)(\partial\gamma/\partial T)$, $\alpha_3 = (2/3a_c)(\partial a_c/\partial T)$, and $\alpha_4 = (1/3n_s)(\partial n_s/\partial T)$, and, of course, $\alpha_A = \alpha_1 + \alpha_2 + \alpha_3 + \alpha_4$. The measurements for γ cited in the previous paragraph give $\alpha_2 = 0.0005$/deg for $T = 30$°C.

TABLE 2 Summary of temperature dependence of structural parameters

Thickness contractivity (α_{Dc})	$(1/D_C)(\partial D_C/\partial T)_\Pi$	0.0019/deg
Head-to-head contractivity (α_{HH})	$(1/D_{HH})(\partial D_{HH}/\partial T)_\Pi$	0.0014/deg
Volume expansivity (α_{Vc})	$(1/V_C)(\partial V_C/\partial T)_\Pi$	0.0010/deg
Area expansivity (α_A)	$(1/A)(\partial A/\partial T)_\Pi$	0.0029/deg
Polymer brush area expansivity (α_A)	$(1/A)(\partial A/\partial T)_\Pi$	0.0032/deg
Molecular area expansion $(\Delta A/\Delta T)_\Pi$	$(\Delta A/\Delta T)_\Pi$	0.21 Å^2/deg

All values are for 30°C.

To evaluate α_3, we use the volume expansion $(\partial V/\partial T)_\Pi = 0.00084$ ml/gm/deg $= 1.1$ Å^3/molecule/deg measured for the gel phase of DSPC (37). In the gel phase, the volume of both chains is $2La_c$, and L is constant because the chains remain extended. Assuming that there is little change in the volume of the headgroups, which are immersed in water, we then have $(\partial a_c/\partial T)/a_c = (\partial V/\partial T)/V_C$, where $V_C = 972$ Å^3 is the volume of the two hydrocarbon chains in DOPC at 30°C (5). This gives $\alpha_3 = 0.0007$/deg for $T = 30$°C.

To evaluate α_4, first note that n_s is defined to be inversely proportional to the persistence length of semiflexible chains, and the temperature dependence of the persistence length is predicted to follow $\exp(\varepsilon_g/kT)$, where ε_g is the difference between the *gauche* and *trans* rotameric energies in hydrocarbon chains (38). This gives $\alpha_4 = (\varepsilon_g/kT)(1/3T)$. Using the accepted value $\varepsilon_g/kT \approx 0.8$, we obtain $\alpha_4 = 0.0009$/deg.

The sum of the preceding four α_i contributions to the area expansivity gives $\alpha_A = 0.0032$/deg, in excellent agreement with our measured value of 0.0029/deg. We may also compare it to the K_C temperature dependence. Since $K_C = K_A(2D_C)^2/24$ and $K_A = 6\gamma$, $(\partial K_C/\partial T)/K_C = 2(\partial D_C/\partial T)/D_C + (\partial\gamma/\partial T)/\gamma$. The value of the lefthand side is -0.0057/deg and the values of the two terms on the right hand side are -0.0038/deg and -0.0015/deg, respectively. If we express the temperature dependence of the hydrocarbon thickness $(\partial D_C/\partial T)/D_C$ as $\exp(\varepsilon_C/kT)$, we obtain $\varepsilon_C/kT = 0.6$, which is satisfyingly close to the rotational isomeric value $\varepsilon_g/kT = 0.8$. It would appear that the polymer brush theory can account very well for our measurement of α_A in DOPC.

A value $\alpha_A = 0.0018$/deg for DOPC at 30°C can be obtained from a study that used the Luzzati method together with an innovative heuristic extrapolation (13). Typical of the Luzzati method in general, this article also reported a larger area, $A = 75$ Å^2, than ours for DOPC at 30°C, as well as larger areas for DMPC and POPC (5).

We next compare our expansivities for DOPC to results obtained for other lipids by other methods. Our value of the molecular area expansion $(\partial A/\partial T)_\Pi = 0.21$ Å^2/deg for DOPC in Table 2 is slightly smaller than the NMR results from Petrache et al. (2), 0.26 Å^2/deg for dilauroylphosphatidylcholine, 0.24 Å^2/deg for DMPC, 0.29 Å^2/deg for dipalmitoylphosphatidylcholine, and 0.27 Å^2/deg for distearoylphosphatidylcholine. However, since the area/molecule, A, is larger for DOPC compared to the saturated chain lipids in that article, their expansivity α_A is larger by a factor of $\sim$1.2 for DMPC, $\alpha_A \approx 0.0036$/deg, than our value for DOPC. As mentioned earlier, α_A increases dramatically in DMPC as the temperature is lowered toward the transition temperature, as can be clearly seen in Needham and Evans (39), who give $\alpha_A = 0.0067$/deg for 5° above the transition and $\alpha_A = 0.0042$/deg for 11° above the transition temperature. This anomalous increase in α_A is not accommodated by the polymer brush theory, which predicts the same values for all four of the α_i contributions to α_A. Nevertheless, the apparent convergence at higher temperatures to the NMR value $\alpha_A \approx 0.0036$/deg suggests that the polymer brush theory is applicable well away from phase transitions. The polymer brush model also does not suggest a difference between the α_A value for unsaturated and saturated chains. The small difference that we obtain for DOPC compared to the values for phosphatidylcholines with saturated chains obtained by NMR may indicate a difference related to the degree of saturation of the hydrocarbon chains, or it may be deemed negligible compared to the experimental uncertainties.

It may also be mentioned that the area expansivity has been investigated by a coarse-grained molecular dynamics simulation (34) that contains two phenomenological parameters σ and ε. We use the separation of chains to estimate $\sigma = 4.8$ Å and we obtain the parameter ε by requiring the area to agree with our experimental area in Fig. 7 of that article. Then, α_A is calculated for the simulation to be 0.0028/deg for DOPC and 0.0055/deg for DMPC. Although this coarse-grained result predicts a stronger dependence upon saturation than the experimental results in the previous paragraph, the number for DOPC is quite close to our value.

Another interesting feature for comparison to other studies is the temperature dependence of bilayer thickness. There are many different measures of bilayer thickness. The two we consider here are 1), the hydrocarbon thickness, $2D_C$, and 2), the head-head distance, D_{HH}, between the peaks in the x-ray EDPs, which is very close to the distance between phosphates on the two monolayers in the bilayer. Because bilayers become thinner with increasing temperature, it is convenient to define contractivities instead of expansivities. Our value for hydrocarbon thickness contractivity, $\alpha_{Dc} = -(\partial(2D_C)/\partial T)_\Pi/(2D_C)$, is 0.0019/deg for DOPC. A somewhat larger value for eggPC, $\alpha_{Dc} = 0.0030$/deg, may be obtained from a low-resolution x-ray study (14). From Table 5 of Petrache et al. (2), we calculate $\alpha_{Dc} = 0.0028$/deg for dilauroylphosphatidylcholine, 0.0025/deg for DMPC, 0.0027/deg for dipalmitoylphosphatidylcholine, and 0.0027 Å/deg for distearoylphosphatidylcholine in the fluid phase, so it appears that for saturated lipids the hydrocarbon contractivity, although similar, may be somewhat greater than for DOPC. Our head-head thickness contractivity, $\alpha_{HH} = -(\partial D_{HH}/\partial T)_\Pi/D_{HH} = 0.0014$/deg for DOPC, is also smaller than the 0.0019/deg for DMPC that can be calculated from Gordeliy et al. (15) or the 0.0022/deg that can be calculated from Simon et al. (14). It can be noted that α_{Dc} should be larger than α_{HH} because the difference in distance between the headgroup peaks and the hydrocarbon region, D_C, does not vary much with temperature, so the temperature derivatives have similar values, but $\alpha_{HH} < \alpha_{Dc}$ because $D_C < D_{HH}$. These contractivities may be helpful to diagnose artifacts in samples or methodology. Using scanning force microscopy on supported phospholipid bilayers, Leonenko et al. (40) reported the temperature dependence of bilayer thickness. For DOPC, their Table 3 shows the thickness increasing by a factor of 2 from 60°C to 22°C, from which one can estimate

their α_{HH} value to be ~0.014/deg for DOPC, far larger than any numbers listed above.

Let us next define the hydrocarbon volume expansivity as $\alpha_{Vc} = (\partial V_C/\partial T)/V_C$, which has the value 0.0010/deg for DOPC at 30°C, taken from a previous volumetric study (9). Then, the relation $V_C = AD_C$ implies $\alpha_{Vc} = \alpha_A - \alpha_{Dc}$, consistent with our results, $\alpha_A = 0.0029$/deg and $\alpha_{Dc} = 0.0019$/deg. Although the major effect of T is to increase A and decrease D_C, volume expansivity contributes 1/3 of the area expansivity. This differs from the suggestion in Simon et al. (14) that the volume expansion is a more minor contributor, but their estimate of the volume expansion was based on volumetric measurements of saturated lipids, and it used α_V rather than α_{Vc} (37). The value $\alpha_{Vc} = 0.0011$/deg for DOPC that can be obtained from Costigan et al. (13) agrees well with our value.

Bilayer interactions

We turn next to the interactions between bilayers and their temperature dependence. The current picture (11) is that there is an attractive van der Waals pressure, P_{vdW}, and two repulsive pressures, the short-range hydration pressure P_{hyd} and the longer-range fluctuation pressure P_{fl}. The average interbilayer water spacing, D'_W, occurs by balancing the sum of these pressures with whatever osmotic pressure is exerted on the system when it is less than fully hydrated. The compression modulus B that we obtain from our x-ray data allows calculation of the fluctuation free energy, F_{fl}, and the corresponding pressure, P_{fl}. Our finding that P_{fl} decays exponentially with D'_W agrees well with theories of soft confinement (17,41) that include the hydration force and the van der Waals force. The soft-confinement theory attempts to add more realistic interactions to the original theory (42), which included only steric interactions. The Helfrich theory (42) rigorously gives a power-law decay, which we do not observe, confirming that soft confinement theory is an improvement. The decay length λ_{fl} for P_{fl} that we report in Table 1 is essentially independent of temperature and agrees with our earlier value, 5.8 Å, which was obtained with different experimental methodology (9). The ratio $\lambda_{fl}/\lambda_{hyd}$ is predicted to be 2 by the soft-confinement theories, but using $\lambda_{hyd} \approx 2.2$ Å together with the values for λ_{fl} in Table 1, it appears that the experimental ratio is significantly larger, a result that also is obtained from Monte Carlo simulations (43). The soft-confinement theory is difficult and requires approximations that apparently reveal themselves in predicting a smaller value for $\lambda_{fl}/\lambda_{hyd}$ than we observe.

Although there is little temperature dependence for the decay length λ_{fl} or for the B modulus, P_{fl} increases with temperature when the water spacing D'_W is kept constant, as can be seen from Eq. 2 with its explicit T dependence and our experimental result that K_C decreases. We did not measure osmotic pressure in this study, so we focused on full hydration where the osmotic pressure is zero. Balancing our new P_{fl} and our previously determined P_{hyd} with P_{vdW} allowed us to obtain the Hamaker parameter, H, for the van der Waals attractive interaction. In our earlier work using only unoriented MLV samples (9), it was only possible to obtain H if a value of K_C was assumed. Table 2 in that article shows that the value of H obtained for 30°C in that study was ~85% as large, assuming $K_C = 7.6 \times 10^{-20}$ J as our new value in Table 1. We now add the new finding that H appears to be essentially constant with temperature for fluid-phase DOPC bilayers; this is consistent with the small 10% decrease in H obtained for gel-phase dibehenoylphosphatidylcholine bilayers over a temperature range of 45°C (14).

The broad picture for the temperature dependence of interactions between DOPC bilayers is essentially the same as that obtained for eggPC (14). The repulsive fluctuation pressure, P_{fl}, increases with increasing temperature and the van der Waals pressure, P_{vdW}, remains constant with temperature for a fixed water spacing, D'_W. The fluctuation pressure decreases more rapidly (exponentially) with increasing D'_W than does the van der Waals pressure (inverse third power), so the bilayers remain bound together in stacks or in MLVs with a finite average D-spacing. Furthermore, this result for the temperature dependence of these two interactions means that at full hydration the average water spacing, D'_W, should increase with increasing temperature, and this is confirmed by our structural results (Table 1). Another of our main structural results is that the bilayer thickness, e.g., D'_B, decreases with increasing temperature. The most easily obtained x-ray result is the fully hydrated repeat spacing D obtained in this study for MLV samples fully immersed in water, but Table 1 shows that $D = D'_B + D'_W$ hardly varies with temperature for DOPC, so results for D alone would obscure the two thermally induced structural changes in D'_B and D'_W that are revealed in our detailed study.

This research was supported by grant GM44976 from the General Medicine Institute of the National Institutes of Health. Synchrotron beam time was provided by the Cornell High Energy Synchrotron Source, which is funded by National Science Foundation grant DMR-0225180.

REFERENCES

1. Rawicz, W., K. C. Olbrich, T. McIntosh, D. Needham, and E. Evans. 2000. Effect of chain length and unsaturation on elasticity of lipid bilayers. *Biophys. J.* 79:328–339.
2. Petrache, H. I., S. W. Dodd, and M. F. Brown. 2000. Area per lipid and acyl length distributions in fluid phosphatidylcholine determined by ^{2}H NMR spectroscopy. *Biophys. J.* 79:3172–3192.
3. Niemelä, P. S., M. T. Hyvönen, and I. Vattulainen. 2006. Influence of chain length and unsaturation on sphingomyelin bilayers. *Biophys. J.* 90:851–863.
4. Triba, M. N., P. F. Devaux, and D. E. Warschawski. 2006. Effects of lipid chain length and unsaturation on bicelle stability. A phosphorus NMR study. *Biophys. J.* 91:1357–1367.
5. Kučerka, N., S. Tristram-Nagle, and J. F. Nagle. 2005. Structure of fully hydrated fluid phase lipid bilayers with monounsaturated chains. *J. Membr. Biol.* 208:193–202.
6. McIntosh, T. J., and S. A. Simon. 2006. Roles of bilayer material properties in function and distribution of membrane proteins. *Annu. Rev. Biophys. Biomol. Struct.* 35:177–198.

7. Botelho, A. V., T. Huber, T. P. Sakmar, and M. F. Brown. 2006. Curvature and hydrophobic forces drive oligomerization and modulate activity of rhodopsin in membranes. *Biophys. J.* 91:4464–4477.
8. Nagle, J. F., and S. Tristram-Nagle. 2000. Structure of lipid bilayers. *Biochim. Biophys. Acta.* 1469:159–195.
9. Tristram-Nagle, S., H. I. Petrache, and J. F. Nagle. 1998. Structure and interactions of fully hydrated dioleoylphosphatidylcholine. *Biophys. J.* 75:917–925.
10. Wiener, M. C., and S. H. White. 1992. Structure of a fluid dioleoylphosphatidylcholine bilayer determined by joint refinement of x-ray and neutron diffraction data. II. Distribution and packing of terminal methyl groups. *Biophys. J.* 61:428–433.
11. Rand, R. P., and V. A. Parsegian. 1989. Hydration forces between phospholipids bilayers. *Biochim. Biophys. Acta.* 988:351–376.
12. Gruner, S. M., M. W. Tate, G. L. Kirk, P. T. S. So, D. C. Turner, and D. T. Keane. 1988. X-ray diffraction study of the polymorphic behavior of *n*-methylated dioleoylphatidylethanolamine. *Biochemistry.* 27:2853–2866.
13. Costigan, S. C., P. J. Booth, and R. H. Templer. 2000. Estimation of lipid bilayer geometry in fluid lamellar phases. *Biochim. Biophys. Acta.* 1468:41–54.
14. Simon, S. A., S. Advani, and T. J. McIntosh. 1995. Temperature dependence of the repulsive pressure between phosphatidylcholine bilayers. *Biophys. J.* 69:1473–1483.
15. Gordeliy, V. I., V. G. Cherezov, and J. Teixeira. 1996. Evidence of the entropic contribution to ''hydration'' forces between membranes. Part II. Temperature dependence of the ''hydration'' force: a small angle neutron scattering study. *J. Mol. Struct.* 383:117–124.
16. Kučerka, N., S. Tristram-Nagle, and J. F. Nagle. 2006. Closer look at structure of fully hydrated fluid phase DPPC bilayers. *Biophys. J.* 90:L83–L85.
17. Podgornik, R., and V. A. Parsegian. 1992. Thermal-mechanical fluctuations of fluid membranes in confined geometries: the case of soft confinement. *Langmuir.* 8:557–562.
18. Kučerka, N., Y. Liu, N. Chu, H. I. Petrache, S. Tristram-Nagle, and J. F. Nagle. 2005. Structure of fully hydrated fluid phase DMPC and DLPC lipid bilayers using x-ray scattering from oriented multilamellar arrays and from unilamellar vesicles. *Biophys. J.* 88:2626–2637.
19. Kučerka, N., J. Pencer, J. N. Sachs, J. F. Nagle, and J. Katsaras. 2007. Curvature effect on the structure of phospholipid bilayers. *Langmuir.* 23:1292–1299.
20. Tristram-Nagle, S. 2007. Preparation of oriented, fully hydrated lipid samples for structure determination using x-ray scattering. *In* Methods in Molecular Biology, Vol. 400. A. M. Dopico, editor. Humana Press, Totowa, NJ. 63–76.
21. Lyatskaya, Y., Y. Liu, S. Tristram-Nagle, J. Katsaras, and J. F. Nagle. 2001. Method for obtaining structure and interactions from oriented lipid bilayers. *Phys. Rev. E Stat. Nonlin. Soft Matter Phys.* 63:011907-1–011907-9.
22. Liu, Y., and J. F. Nagle. 2004. Diffuse scattering provides material parameters and electron density profiles of biomembranes. *Phys. Rev. E Stat. Nonlin. Soft Matter Phys.* 69:040901-1–040901-4.
23. De Gennes, P. G., and J. Prost. 1993. The Physics of Liquid Crystals. Oxford University Press, Oxford, UK.
24. Petrache, H. I., N. Gouliaev, S. Tristram-Nagle, R. Zhang, R. M. Suiter, and J. F. Nagle. 1998. Interbilayer interactions from high-resolution x-ray scattering. *Phys. Rev. E Stat. Phys. Plasmas Fluids Relat. Interdiscip. Topics.* 57:7014–7024.
25. Klauda, J. B., N. Kučerka, B. R. Brooks, R. W. Pastor, and J. F. Nagle. 2006. Simulation-based methods for interpreting x-ray data from lipid bilayers. *Biophys. J.* 90:2796–2807.
26. Tristram-Nagle, S., Y. Liu, J. Legleiter, and J. F. Nagle. 2002. Structure of gel phase DMPC determined by x-ray diffraction. *Biophys. J.* 83: 3324–3335.
27. Greenwood, A. I., S. Tristram-Nagle, and J. F. Nagle. 2006. Partial molecular volumes of lipids and cholesterol. *Chem. Phys. Lipids.* 143:1–10.
28. Koenig, B. W., and K. Gawrisch. 2005. Specific volumes of unsaturated phosphatidylcholines in the liquid crystalline lamellar phase. *Biochim. Biophys. Acta.* 1715:65–70.
29. Reference deleted in proof.
30. Liu, Y. 2003. New method to obtain structure of biomembranes using diffuse x-ray scattering: application to fluid phase DOPC lipid bilayers. Ph. D. thesis. Carnegie Mellon University, Pittsburgh, Pennsylvania.
31. Parsegian, V. A. 2006. Van der Waals Forces: A Handbook for Biologists, Chemists, Engineers, and Physicists. Cambridge University Press, New York.
32. Niggemann, G., M. Kummrow, and W. Helfrich. 1995. The bending rigidity of phosphatidylcholine bilayers: dependence on experimental method, sample cell sealing and temperature. *J. Phys. II France.* 5: 413–425.
33. Zeppieri, S., J. Rodríguez, and A. L. L. de Ramos. 2001. Interfacial tension of alkane + water systems. *J. Chem. Eng. Data.* 46:1086–1088.
34. Stevens, M. J. 2004. Coarse-grained simulations of lipid bilayers. *J. Chem. Phys.* 121:11942–11948.
35. Chu, N., N. Kučerka, Y. Liu, S. Tristram-Nagle, and J. F. Nagle. 2005. Anomalous swelling of lipid bilayer stacks is caused by softening of the bending modulus. *Phys. Rev. E Stat. Nonlin. Soft Matter Phys.* 71:041904-1–041904-8.
36. Lewis, R. N. A. H., B. D. Sykes, and R. McElhaney. 1988. Thermotropic phase-behavior of model membranes composed of phosphatidylcholines containing cis-monounsaturated chain homologs of oleic acid-differential scanning calorimetry and ^{31}P NMR spectroscopic studies. *Biochemistry.* 27:880–887.
37. Nagle, J. F., and D. A. Wilkinson. 1978. Lecithin bilayers density measurements and molecular interactions. *Biophys. J.* 23:159–175.
38. De Gennes, P. G. 1979. Scaling concepts in polymer physics. Cornell University Press, Ithaca, NY.
39. Needham, D., and E. Evans. 1988. Structure and mechanical properties of giant lipid (DMPC) vesicle bilayers from 20°C below to 10°C above the liquid crystal-crystalline phase transition at 24°C. *Biochemistry.* 27: 8261–8269.
40. Leonenko, Z. V., E. Finot, H. Ma, T. E. S. Dahms, and D. T. Cramb. 2004. Investigation of temperature-induced phase transition in DOPC and DPPC phospholipid bilayers using temperature-controlled scanning force microscopy. *Biophys. J.* 86:3783–3793.
41. Evans, E., and D. Needham. 1987. Physical properties of surfactant bilayer membranes: thermal transitions, elasticity, cohesion, and colloidal interactions. *J. Phys. Chem.* 91:4219–4228.
42. Helfrich, W. 1978. Steric interaction of fluid membranes in multilayer systems. *Z. Naturforsch. A.* 33:305–315.
43. Gouliaev, N., and J. F. Nagle. 1998. Simulations of interacting membranes. *Phys. Rev. Lett.* 81:2610–2613.